American Mineralogist, Volume 81, pages 1126–1132, 1996

Transmission electron microscopy study of the thermal decomposition of tremolite into clinopyroxene

HUIFANG XU,[1,*] DAVID R. VEBLEN,[1] GUFENG LUO,[2] AND JIYUE XUE[2]

[1]Department of Earth and Planetary Sciences, Johns Hopkins University, Baltimore, Maryland 21218, U.S.A.
[2]Department of Earth Sciences, Nanjing University, Nanjing, Jiangsu 210093, People's Republic of China

ABSTRACT

In situ–heating transmission electron microscopy and high-resolution transmission electron microscopy studies of the thermal decomposition of tremolite show that transformed pyroxenes have $C2/c$ and $P2_1/c$ structures and retain axial orientation of the tremolite structure with $I2/m$ orientation. Amorphous silica forms only on the surface of the heated crystals.

Thermal decomposition of tremolite, which takes place at 740 °C, is characterized by the formation of (010) clinopyroxene slabs with thicknesses of 18 and 36 Å along the b axis. The (010) slabs with $C2/c$ symmetry are coherent with the tremolite matrix. Heated tremolite with (010) slabs has the same composition as "anhydrous tremolite." Clinopyroxene domains formed at 780 °C are composed of $C2/c$ and $P2_1/c$ clinopyroxenes with an exsolution lamella-like texture. The products characterized by clinopyroxene domains are isolated by tremolite with (010) clinopyroxene slabs. The bulk composition of transformed clinopyroxenes is almost the same as that of anhydrous tremolite. The structure of the clinopyroxenes with stoichiometry $(Ca,Mg)_7Si_8O_{23}$ can be considered to be the pyroxene structure with a random distribution of (Ca,Mg)O vacancies in the octahedral bands. The clinopyroxenes with (Ca,Mg)O vacancies are thermodynamically unstable. The texture consisting of pyroxene chains in multiples of four within the amphibole matrix may indicate a dehydration reaction of amphibole, rather than hydration of pyroxene. Further annealing of the heated specimen at higher temperature increases the concentration of Ca cations in $C2/c$ clinopyroxene and results in coarser clinopyroxene lamellae.

Transformed clinopyroxene with only $P2_1/c$ symmetry, described by Freeman and Taylor (1960), is an artifact of overlapping single-crystal X-ray diffraction patterns of $C2/c$ and $P2_1/c$ structures. The transformation product of one diopside-like clinopyroxene, described by Wang and Zhang (1991), results from weak diffraction spots violating the C-centered lattice structure that did not appear in X-ray powder diffraction patterns.

INTRODUCTION

The thermal decomposition of amphiboles into pyroxenes is a reaction that occurs in contact metamorphic rocks (e.g., mafic hornfels and calcareous hornfels) from amphibolite facies to pyroxene facies (Williams et al. 1958) and in some intermediate acidic volcanic rocks (e.g., hornblende-andesite) (Williams et al. 1958; Johannsen 1937). For instance, dark rims around hornblende in hornblende-andesites are composed of magnetite, clinopyroxene, and orthopyroxene (Johannsen 1937). Akai et al. (1985) observed disordered (010) pyroxene slabs in a natural oxyhornblende by means of transmission electron microscopy (TEM). They suggested that the disordered (010) pyroxene slabs were produced by dehydroxylation of primary hornblende. The decomposition reaction takes place in hornfels under nonoxidizing conditions, whereas in andesitic rocks the reaction proceeds under oxidizing conditions and is accompanied by the formation of iron oxides (e.g., magnetite). The former reaction may be represented as amphibole → pyroxenes + silica; and the reaction for the latter case may be represented as amphibole → pyroxenes + silica + iron oxides. Therefore, the study of the thermal decomposition of amphibole may help to elucidate the microscopic mechanism of the transformation from amphibole into pyroxene in natural rocks.

The dehydration and decomposition of amphibole under nonoxidizing and oxidizing conditions have been studied by means of X-ray diffraction (XRD) and optical microscopy, especially for Na-bearing alkali amphiboles (Addison et al. 1962a, 1962b; Addison and Sharp 1962; Hodgson et al. 1965; Patterson 1965; Tomita 1965; Patterson and O'Connor 1966; Clark and Freeman 1967; Freeman and Frazer 1968; Ernst and Wai 1970). Free-

* Present address: Department of Geology and Center for Solid State Science, Arizona State University, Tempe, Arizona 85287-1404, U.S.A.

0003–004X/96/0910–1126$05.00

man and Taylor (1960) investigated the dehydration and decomposition of tremolite into pyroxene with the use of single-crystal X-ray diffraction methods. Their results show that the pyroxene phase appears at 700 °C and retains axial orientation with the amphibole in the $I2/m$ orientation. They also reported that the pyroxene product has $P2_1/c$ symmetry. On the basis of thermal analysis, Ivanova and Kasatov (1974) proposed clinoenstatite, diopside, and cristobalite as the decomposition products of tremolite. Recently, using X-ray powder diffraction, Wang and Zhang (1991) found noncrystalline silica and one diopside-like clinopyroxene in a heated tremolite. Their results also show that tremolite is stable below 800 °C. The decomposition of grunerite in nonoxidizing conditions at 775 °C results in the formation of clinoferrosilite and amorphous silica (Ghose and Weidner 1971). An in situ–heating TEM study of an actinolite showed that decomposition takes place at 770 °C (Xu et al. 1988). These studies confirm that the decomposition temperature of different amphiboles ranges from 700 to over 800 °C. To reveal the structure, composition, and microstructure of the clinopyroxene products at the unit-cell scale, we present the results of in situ–heating and high-temperature annealing TEM experiments, and high-resolution transmission electron microscopy (HRTEM) of the thermal decomposition of a tremolite into clinopyroxenes.

Sample and experiment

The sample used in this study is a tremolite crystal of the Mineralogy Laboratory of Nanjing University. For in situ TEM investigation the specimen was mounted on a molybdenum grid and removed from the petrographic thin section of the tremolite in the (100) orientation. Then the specimen was thinned by ion milling to make it suitable for TEM investigation.

The unheated specimen was investigated by TEM using a double-tilt specimen stage. In situ–heating experiments were performed on a JEOL 200CX transmission electron microscope equipped with a single-tilt heating stage like that used in the decomposition of an actinolite (Xu et al. 1988). The b axis of the tremolite was oriented with the tilt axis of the heating stage, so that features along the b axis could be observed while tilting the crystal. The rate of temperature increase of the stage furnace was about 10 °C/min from room temperature to 700 °C, and 3 °C/min from 700 to 780 °C. After the temperature reached 780 °C, the specimen was cooled to room temperature in the microscope column. Then the specimen was transferred to a double-tilt specimen stage for HRTEM investigations.

To reveal microstructures normal to the c axis, tremolite chips with cutting surface normal to the c axis were also selected for the investigation. These specimens are as follows: (1) tremolite heated at 740 °C for 1 h; (2) tremolite heated at 780 °C for 1 h; (3) tremolite heated at 960 °C for 10 h. All the specimens were quenched to room temperature in air. Petrographic thin sections were prepared from the quenched chips, and TEM specimens were selected from the central parts of the thin sections. Therefore, all the specimens in the TEM study were from central parts of the annealed crystals.

TEM and analytical electron microscopy (AEM) investigations of the annealed specimens were performed on a Philips 420 TEM equipped with an energy-dispersive X-ray detector and a Princeton-Gamma Tech analyzer as described by Veblen and Bish (1988) and Livi and Veblen (1987). Operating voltage was 120 kV. Chemical formulas of the tremolite and pyroxenes were calculated on the basis of 23 and six O atoms, respectively. A representative chemical formula of the tremolite calculated from the AEM analysis is $(Ca_{1.94}Na_{0.20}K_{0.04})_{2.18}(Mg_{4.69}Fe_{0.07}Al_{0.12}Mn_{0.04})_{4.92}[(Si_{7.88}Ti_{0.01}Al_{0.11})_8O_{22}](OH)_2$.

Results and discussion

TEM results

Selected-area electron diffraction (SAED) patterns of the tremolite show sharp diffraction spots (Figs. 1a and 2a). The results indicate there is no chain-width disorder in the tremolite. In situ–heating TEM studies show that there are no changes in the diffraction pattern and its corresponding images when the sample is heated from room temperature to about 740 °C. The lack of changes in the diffraction pattern indicates that transformation of amphibole chains into pyroxene chains does not occur below 740 °C, or that the transformation rate is not as fast as the rapid heating rate used. As the temperature was raised to 740 °C, weak streaking along the b^* axis was observed in the [100] zone-axis diffraction patterns (Fig. 1b). The streaked diffraction spots indicate chain-width disorder in the tremolite. A [001] zone-axis SAED from a quenched tremolite at 740 °C also shows streaking along the b^* direction (Fig. 2b). Strong streaking appears on some positions of the [001] zone-axis pattern (Fig. 2b). Sharp diffraction spots in Figure 2b are from the tremolite and transformed clinopyroxene. However, all the streaked diffraction spots are only from very narrow slabs of pyroxene chains in the quenched crystal. As the annealing temperature was increased further, the intensity of the streaking increased, and the intensity of the main Bragg reflections changed in [100] and [001] zone-axis SAED patterns.

Figure 1c, a [100] zone-axis SAED pattern of the specimen heated in situ at 780 °C, shows overlapping diffraction patterns of a [100] zone axis of tremolite and a [101] zone axis of clinopyroxene (Figs. 1c and 1e). By tilting the specimen about 30°, overlapping diffraction patterns from the [101] zone axis of tremolite and the [100] zone axis of clinopyroxene were obtained (Fig. 1d). Some extra spots in the SAED pattern (Fig. 1d) are from multiple diffraction owing to the overlap of tremolite and clinopyroxene. The micrograph negative shows that there is a very weak and diffuse diffraction ring with an average d value of 2.5 Å, which is from amorphous silica as described by Freeman and Taylor (1960) and Ghose and Weidner (1971). After the in situ–heated tremolite was

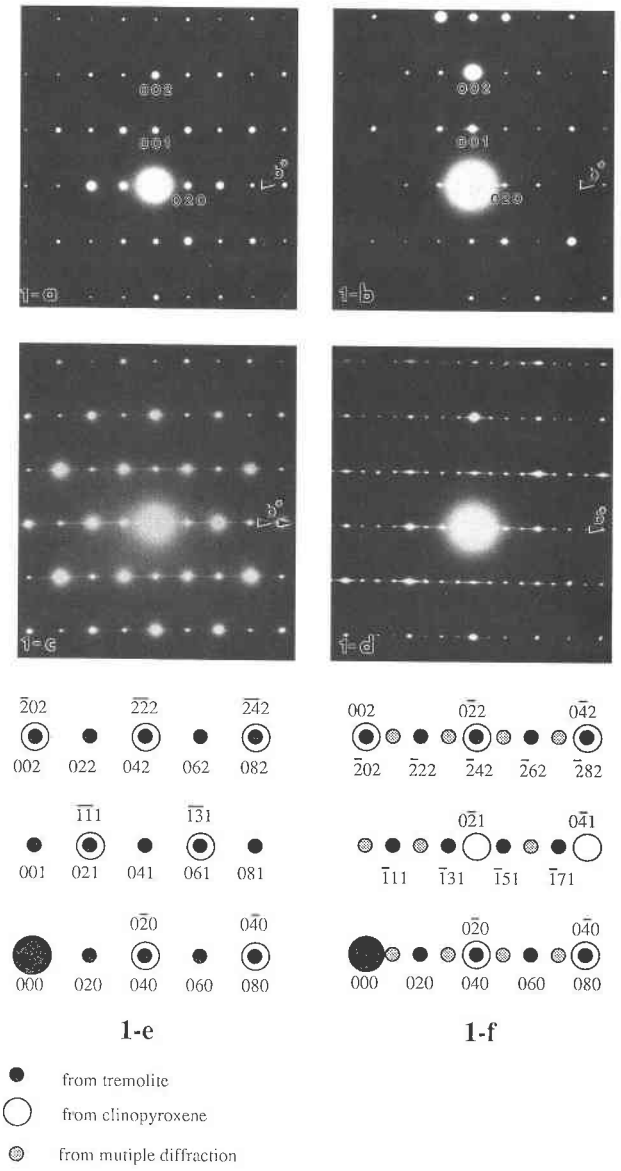

Figure 1. Electron diffraction patterns of the tremolite before heating (**a**), heated in situ at 740 °C (**b**), and heated in situ at 780 °C (**c** and **d**). The [100] zone-axis SAED patterns are shown in **a** and **b**; **c** shows overlapping SAED patterns from the [100] zone axis of the tremolite and the [101] zone axis of product clinopyroxene; and **d** shows overlapping diffraction patterns from the [101] zone axis of the tremolite and the [100] zone axis of product clinopyroxene. Some additional spots in **d** are from multiple diffraction owing to the overlap of the tremolite and clinopyroxene. The indices of diffraction spots of SAED patterns **c** and **d** are illustrated in **e** and **f**, respectively, in which the spots with labeled indices above them are from clinopyroxene, and the spots with labeled indices below them are from tremolite. Labels and indices of the diffraction spots for tremolite are based on the *C*2/*m* amphibole orientation.

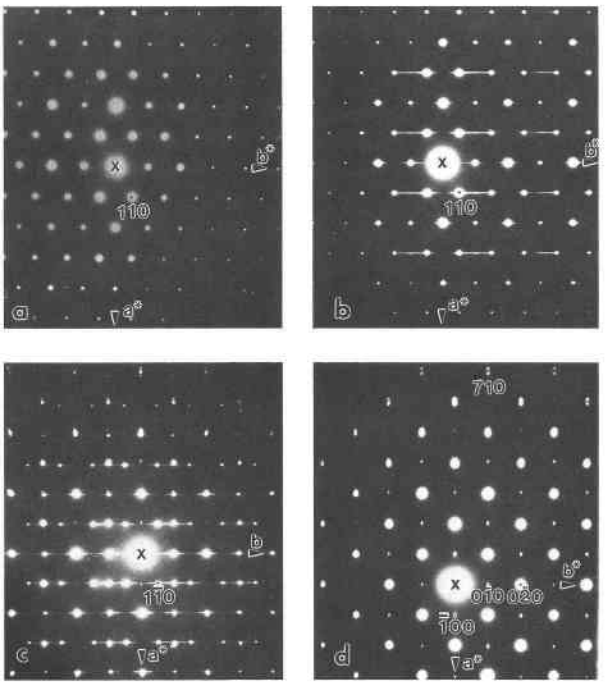

Figure 2. The [001] zone-axis SAED patterns of unheated tremolite (**a**) and tremolite quenched from 740 °C (**b**), 780 °C (**c**), and 960 °C (**d**). Labels and indices of the diffraction spots for the tremolite are based on *C*2/*m* amphibole orientation. In the SAED patterns with both tremolite and product clinopyroxene, the relationship between a^* of tremolite with *C*2/*m* setting and a^* of the clinopyroxene is $a^*_{Tr} = -a^*_{Cpx}$.

rethinned by Ar ion milling, the diffuse ring disappeared. It can thus be inferred that the amorphous silica that causes the diffuse diffraction ring occurs only on the surface of the specimen. A [001] zone-axis SAED pattern from a specimen quenched from 780 °C shows streaking along the b^* direction and additional spots for clinopyroxenes (Fig. 2c). It can be seen in Figure 2c that there are two kinds of clinopyroxenes with two d_{100} values. The set of diffraction maxima with larger d_{100} is from *C*2/*c* clinopyroxene. The other set of diffraction maxima with smaller d_{100}, which violates the *C*-centered lattice structure, is from $P2_1/c$ clinopyroxene. The difference between the d_{100} values of *C*2/*c* clinopyroxene and $P2_1/c$ clinopyroxene is more obvious in the SAED pattern from a specimen quenched from 960 °C (Fig. 2d). From these SAED patterns, the orientation relationship between tremolite (Tr) and clinopyroxene (Cpx) products is $a_{Cpx} = [\bar{1}0\bar{1}]_{Tr}$, $b_{Cpx} = -(\frac{1}{2})b_{Tr}$, $c_{Cpx} = c_{Tr}$, and $a^*_{Tr} = -a^*_{Cpx}$.

A dark-field image of the tremolite quenched from 740 °C, produced by selecting a streaked diffraction spot corresponding to a 110 reflection of the *C*2/*c* clinopyroxene, shows (010) slabs within the tremolite matrix (Fig. 3). An HRTEM image shows that these slabs are clinopyroxene chains with thicknesses of 18 and 36 Å along the *b* axis (Fig. 4). The boundaries between the pyroxene slabs and the tremolite matrix are coherent. Figure 5 shows schematically the boundary relationship between a clinopyroxene slab and tremolite matrix (area A) and the termination of a clinopyroxene slab within the tremolite matrix (area B). Most clinopyroxene slabs with a thickness of 18 Å (corresponding to four pyroxene chains) are

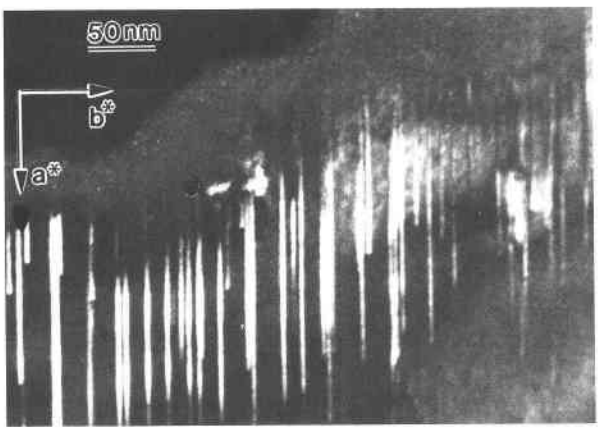

FIGURE 3. A dark-field image of tremolite quenched from 740 °C produced by selecting a streaked diffraction maxima at 110*, showing (010) clinopyroxene slabs.

the decomposition products of two amphibole chains (Figs. 4 and 5). From the streaking and HRTEM image of Figure 4, it can be inferred that the pyroxene slabs have *C*-centered lattice structure and that *C*2/*c* is the probable symmetry for the slabs. The clinopyroxene slabs with thicknesses of 18 or 36 Å are coherent with the matrix structure of tremolite. AEM analysis does not show any compositional difference between the heated and unheated tremolite crystals. The composition of the clinopyroxene slabs intergrown with tremolite may be the same as that of anhydrous tremolite, i.e., $(Ca,Mg)_7Si_8O_{23}$. The clinopyroxene slabs are rich in SiO_2 [or deficient in (Ca,Mg)O] in comparison with the normal pyroxene stoichiometry. It was observed that the clinopyroxene slabs became amorphous under electron-beam radiation much faster than the remaining tremolite. In general, pyroxene is more stable than amphibole under electron-beam radiation. It can be inferred that the clinopyroxene slabs with (Mg,Ca)O deficiencies in octahedral sites are less stable than normal pyroxene and tremolite structures.

A typical bright-field image (Fig. 6) of the tremolite quenched from 780 °C shows tremolite with clinopyroxene slabs, and coarser, isolated clinopyroxene domains.

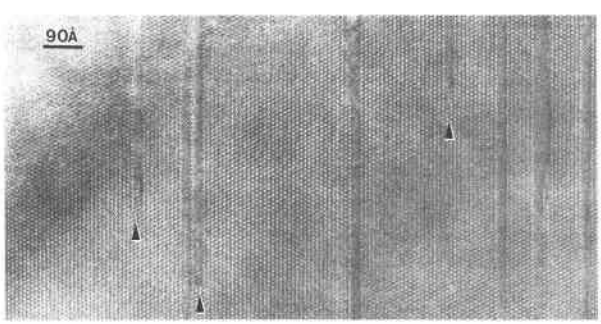

FIGURE 4. HRTEM image of tremolite quenched from 740 °C, showing (010) clinopyroxene slabs with thicknesses of 18 and 36 Å along the *b* axis. Arrows indicate terminations of clinopyroxene slabs.

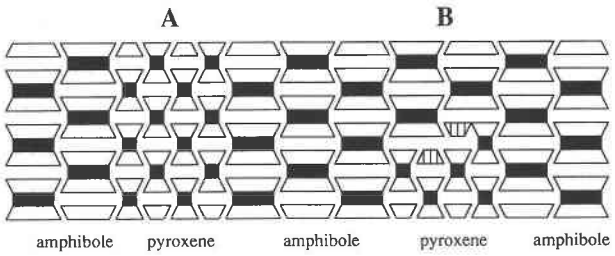

FIGURE 5. A schematic interpretation of a clinopyroxene slab with a thickness of four clinopyroxene chains along the *b* axis (area A) and termination of a clinopyroxene slab (area B).

An SAED pattern from the tremolite with (010) slabs shows the same phenomena as tremolite quenched from 740 °C (Fig. 7a). An SAED pattern from a coarser clinopyroxene domain shows overlapping diffraction patterns from two clinopyroxenes with different d_{100} values (Fig. 7b). One diffraction set has a *C*-centered lattice structure (i.e., *C*2/*c* symmetry). The other diffraction set with a smaller d_{100} displays additional weak reflections that violate the *C*-centered lattice structure (Fig. 7b). Figure 7b indicates that part of the coarser clinopyroxene domain has space group $P2_1/c$ as indicated by Freeman and Taylor (1960). The (100) lamellar contrast in the coarser clinopyroxene domain (Fig. 6) may indicate clinopyroxene lamellae with *C*2/*c* and $P2_1/c$ symmetries. An HRTEM image shows a coarser clinopyroxene domain isolated by tremolite with (010) slabs (Fig. 8). The boundary between the coarser clinopyroxene and tremolite is almost coherent. No APB-like texture in the isolated clinopyroxene domains was observed. It is possible that these *C*2/*c* and $P2_1/c$ clinopyroxenes formed during the decomposition of tremolite at high temperature. The

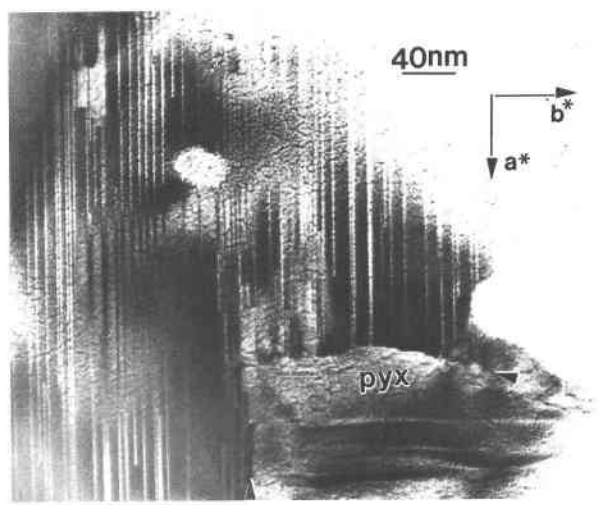

FIGURE 6. Bright-field image of tremolite quenched from 780 °C, showing a coarser clinopyroxene (pyx) within the tremolite with thin clinopyroxene slabs. Arrows indicate the boundaries between a coarser clinopyroxene domain and the tremolite matrix. Labels of *a** and *b** refer to the tremolite with *C*2/*m* setting.

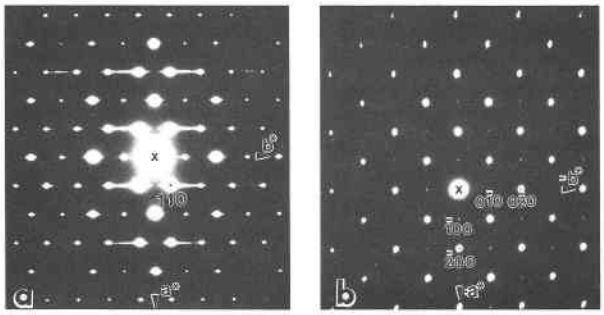

FIGURE 7. (a) SAED pattern from tremolite matrix with (010) clinopyroxene slabs, showing sharp diffraction maxima from the tremolite and transformed clinopyroxene slabs and streaking from transformed clinopyroxene slabs only. (b) SAED pattern from a coarser clinopyroxene domain, showing two sets of diffraction spots characterizing clinopyroxenes with C-centered and primitive lattice structures, respectively. The relationship between a^* of tremolite with $C2/m$ setting and a^* of the clinopyroxene is $a^*_{Tr} = -a^*_{Cpx}$.

formation of the lamellar texture in the clinopyroxene domains may involve segregation of Ca and Mg atoms into $C2/c$ and $P2_1/c$ clinopyroxenes.

AEM analysis of the tremolite heated at 780 °C does not show any obvious compositional difference between isolated clinopyroxene domains and tremolite with (010) clinopyroxene slabs. The transformed clinopyroxene domains are also SiO_2 rich, or (Ca,Mg)O deficient. Therefore, if H_2O is not considered, the transformation of tremolite to clinopyroxene is similar to an isochemical

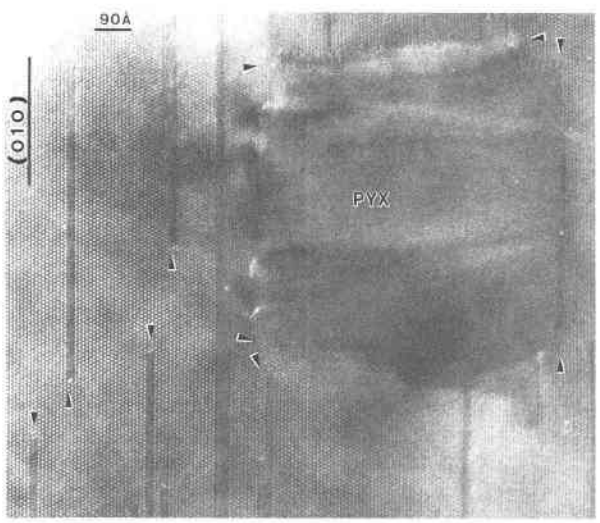

FIGURE 8. HRTEM image of the tremolite heated at 780 °C, showing a coarser clinopyroxene (PYX) domain isolated by the tremolite with clinopyroxene slabs. The isolated domain shows a lamella-like texture. Some areas show weak {110} lattice fringes. Arrows indicate terminations of clinopyroxene slabs and the boundaries between the pyroxene domain and the tremolite matrix.

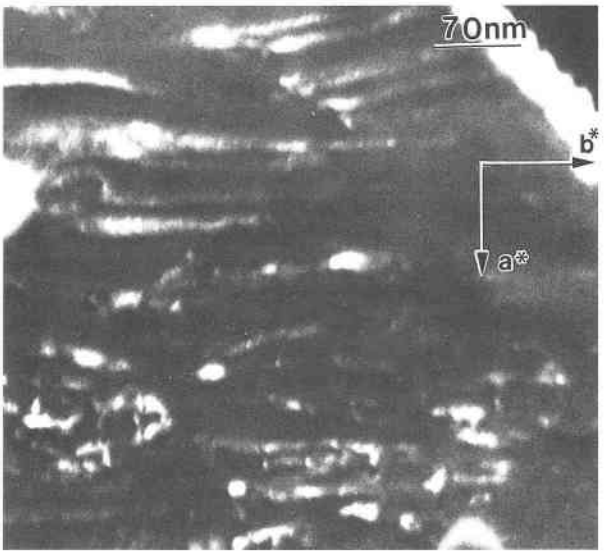

FIGURE 9. A dark-field image (**g** = 100) of clinopyroxene transformed from tremolite at 960 °C, showing a lamella-like texture resulting from segregation of Ca and Mg between areas having $C2/c$ and $P2_1/c$ symmetries, respectively.

reaction. Its structure may be considered to be that of normal clinopyroxene with a random distribution of (Ca,Mg)O vacancies in the octahedral sites. The difference between transformed clinopyroxene domains and (010) slabs is that both $C2/c$ and $P2_1/c$ structures occur in the domains and only the $C2/c$ structure occurs in the slabs.

The tremolite quenched from 960 °C contains only $C2/c$ and $P2_1/c$ clinopyroxenes. A dark-field image produced by selecting a diffracted beam (**g** = 100) from $P2_1/c$ pyroxene (i.e., a diffraction spot with smaller d_{001}) shows wormlike exsolution lamellae nearly parallel to (100) (Fig. 9). These diffraction maxima with $h + k$ = odd in the SAED pattern (Fig. 2d) result from the clinopyroxene lamellae that violate the C-centered lattice structure. A tilted SAED pattern with the first-order Laue zone shows that there are no diffraction maxima characterizing the 18 Å periodicity along the a^* direction in the $hk1$ diffraction zone (Fig. 10). The above results also indicate that the pyroxene lamellae violate a C-centered structure and have $P2_1/c$ symmetry, rather than *Pbca* (orthopyroxene) symmetry. AEM results indicate that the clinopyroxene lamellae have different compositions. The chemical formulas of $C2/c$ clinopyroxene and $P2_1/c$ clinopyroxene, calculated from AEM analyses based on six O atoms, are $(Ca_{0.89}Na_{0.17}K_{0.02})_{1.08}(Mg_{0.84}Fe_{0.03}Al_{0.07}Mn_{0.02})_{0.96}[Si_{2.00}O_6]$ and $(Ca_{0.26}Na_{0.01}K_{0.02})_{0.29}(Mg_{1.46}Fe_{0.01}Mn_{0.01})_{1.48}[Si_{2.12}O_6]$, respectively. $P2_1/c$ clinopyroxene is relatively rich in Mg, and $C2/c$ clinopyroxene is relatively rich in Ca. $P2_1/c$ clinopyroxene is also rich in SiO_2. HRTEM images of the clinopyroxenes show coherent boundaries between $C2/c$ pyroxene lamellae (C) and $P2_1/c$ pyroxene lamellae (P) (Fig. 11). There is also no APB-like texture resulting from

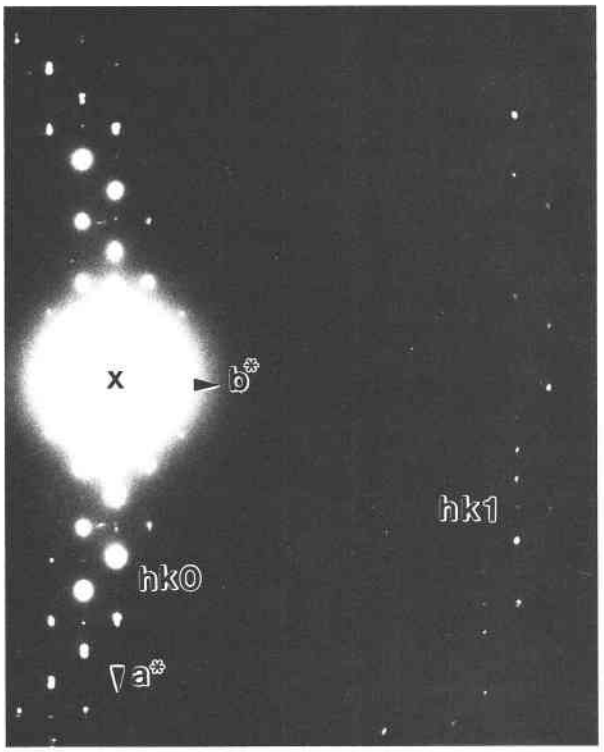

FIGURE 10. A nearly [001] zone-axis SAED pattern of the clinopyroxene, showing zero-order and first-order Laue-zone diffraction maxima. The diffraction pattern does not indicate an 18 Å periodicity along the a^* direction in the first-order Laue zone.

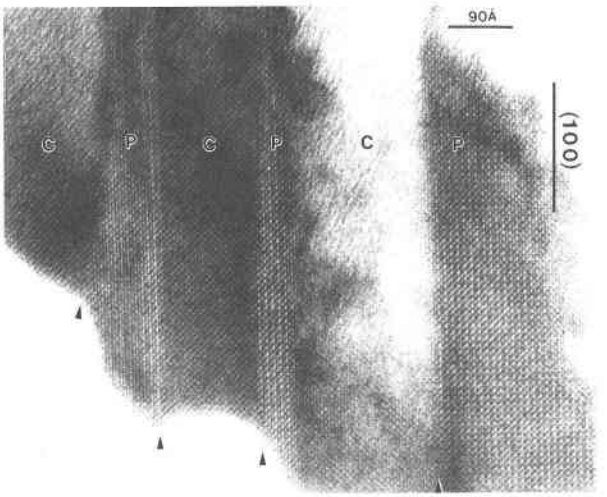

FIGURE 11. An HRTEM image of clinopyroxene, showing $C2/c$ (C) and $P2_1/c$ (P) clinopyroxene lamellae with coherent boundaries. The boundaries are nearly parallel to (100) of the pyroxene structure.

a $C2/c \rightarrow P2_1/c$ phase transition in clinopyroxene. Presumably, the exsolution lamella-like texture formed during the decomposition of tremolite, and the segregation of Ca and Mg atoms occurred at high temperature rather than from exsolution during quenching of the specimen, because there is a wide miscibility gap between diopside and Mg-rich pyroxene at 960 °C (Huebner 1980).

On the basis of our TEM results, we conclude that the solid-state transformation products of tremolite are both $C2/c$ and $P2_1/c$ clinopyroxenes. It can be inferred that clinopyroxene with only $P2_1/c$ symmetry, described by Freeman and Taylor (1960), is an artifact of overlapping diffraction patterns of $C2/c$ and $P2_1/c$ structures in their single-crystal XRD study. Similarly, one diopside-like clinopyroxene described by Wang and Zhang (1991) results from weak diffraction spots violating the C-centered lattice structure that did not appear in X-ray powder diffraction.

Mechanism of the transformation

HRTEM images of the tremolite specimens quenched from 740 and 780 °C show that the (010) clinopyroxene slabs with thicknesses of 18 and 36 Å along the b axis correspond to the dimensions of two or four tremolite chains along the b axis. There are always multiples of four pyroxene chains (i.e., 4, 8, 12, etc.) within the tremolite matrix, unlike in altered pyroxenes with chain-width disorder (Nakajima and Ribbe 1980; Veblen and Buseck 1981; Veblen and Bish 1988; Griffin et al. 1985). In this case, the only way to match the structures between the amphibole chains and the product pyroxene chains, during the solid-state transformation of tremolite into pyroxene, is by breaking every two amphibole chains to form four pyroxene chains (Fig. 5), according to the rules for coherent termination of pyribole chains (Veblen and Buseck 1980). The decomposition of two amphibole chains into four pyroxene chains occurs by rearrangement of Si-O tetrahedra and interdiffusion of Ca and Mg atoms within (100) octahedral bands. The diffusion could be enhanced by the presence of H_2O released in the dehydration reaction. Coarsening of pyroxene slabs and domains could be achieved by further growth of pyroxene slabs and domains along the a, b, and c axes. The dehydration of tremolite is different from the hydration of pyroxene and amphibole involving hydrothermal solutions, which was described by Veblen and Buseck (1980, 1981) and Veblen (1991). The formation of the exsolution lamella-like texture in the transformed clinopyroxenes results from further segregation of Ca and Mg atoms in the $C2/c$ and $P2_1/c$ clinopyroxenes, and this texture is similar to the early-stage exsolution textures in pyroxenes (Nord et al. 1976; Buseck et al. 1980).

ACKNOWLEDGMENTS

We thank Junji Akai, Michael Czank, and Adrian Brearley for their critical reviews and helpful comments. This work was supported by NSF grant EAR-8903630 and NSF of China. Electron microscopy was performed in the Johns Hopkins University HRTEM laboratory, established with partial support from NSF grant EAR-8300360, and the Laboratory of Solid State Microstructures of Nanjing University.

References cited

Addison, C.C., Addison, W.E., Neal, G.H., and Sharp, J.H. (1962a) Amphiboles: I. The oxidation of crocidolite. Journal of Chemical Society, 278, 1468–1471.

Addison, C.C., Neal, G.H., and Sharp, J.H. (1962b) Amphiboles: II. The kinetics of the oxidation of crocidolite. Journal of Chemical Society, 279, 1472–1475.

Addison, C.C., and Sharp, J.H. (1962) Amphiboles: III. The reduction of crocidolite. Journal of Chemical Society, 716, 3693–3698.

Akai, J., Tomita, K., and Yamaguchi, Y. (1985) High resolution electron microscopic observation of pyroxene lamellae in oxyhornblende. Earth Science, 38, 334–345.

Buseck, P.R., Nord, G.L., Jr., and Veblen, D.R. (1980) Subsolidus phenomena in pyroxenes. In Mineralogical Society of America Reviews in Mineralogy, 7, 117–211.

Clark, M.W., and Freeman, A.G. (1967) Kinetics and mechanism of dehydroxylation of crocidolite. Transactions of Faraday Society, 63(536), 2051–2056.

Ernst, W.G., and Wai, C.M. (1970) Infrared, X-ray and optical study of cation ordering and dehydrogenation in natural and heat-treated sodic amphiboles. American Mineralogist, 55, 1226–1258.

Freeman, A.G., and Taylor, F.H.W. (1960) Die Entwasserung von Tremolit. Silikattechnik, 11, 390–392.

Freeman, A.G., and Frazer, F.W. (1968) A pseudo-polymorphic transition: The amphibole to pyroxene reaction. Nature, 220, 67–68.

Ghose, H., and Weidner, J.R. (1971) Oriented transformation of grunerite to clinoferrosilite at 775 °C and 500 bar argon pressure. Contributions to Mineralogy and Petrology, 30, 64–71.

Griffin, W.L., Mellini, M., Oberti, R., and Rossi, G. (1985) Evolution of coronas in Norwegian anorthites: Re-evaluation based on crystal-chemistry and microstructures. Contributions to Mineralogy and Petrology, 91, 330–339.

Hodgson, A.A., Freeman, A.G., and Taylor, F.H.W. (1965) The thermal decomposition of crocidolite from Koegas, South Africa. Mineralogical Magazine, 35, 5–30.

Huebner, J.S. (1980) Pyroxene phase equilibria at low pressure. In Mineralogical Society of America Reviews in Mineralogy, 7, 213–288.

Ivanova, V.P., and Kasatov, B.K. (1974) Thermal analysis of minerals and rocks, p. 30–211. Mineral Resources, Leningrad (in Russian).

Johannsen, A. (1937) A descriptive petrology of the igneous rocks, vol. III: The intermediate rocks, p. 160–172. University of Chicago Press, Illinois.

Livi, K.J.T., and Veblen, D.R. (1987) "Eastonite" from Easton, Pennsylvania: A mixture of phlogopite and a new form of serpentine. American Mineralogist, 72, 113–125.

Nakajima, Y., and Ribbe, P.H. (1980) Alteration of pyroxenes from Hokaido, Japan, to amphibole, clays and other biopyriboles. Neues Jahrbuch für Mineralogie Monatshefte, 6, 258–268.

Nord, G.L., Heuer, A.H., and Lally, J.S. (1976) Pigeonite exsolution from augite. In H.-R. Wenk, Ed., Electron microscopy in mineralogy, p. 220–227. Springer-Verlag, Berlin.

Patterson, J.H. (1965) The thermal disintegration of crocidolite in air and in vacuum. Mineralogical Magazine, 35, 31–37.

Patterson, J.H., and O'Connor, J.J. (1966) Chemical studies of amphibole asbestos: I. Structural changes of heat-treated crocidolite, amosite and tremolite from infrared absorption studies. Australian Journal of Chemistry, 19, 1155–1164.

Tomita, K. (1965) Studies on oxyhornblende. Memoranda of College of Science, University of Kyoto, series B, 32, 37–87.

Veblen, D.R. (1991) Polysomatism and polysomatic series: A review and applications. American Mineralogist, 76, 801–826.

Veblen, D.R., and Buseck, P.R. (1980) Microstructures and reaction mechanisms in biopyribole. American Mineralogist, 65, 599–623.

——— (1981) Hydrous pyriboles and sheet silicates in pyroxenes and uralites: Intergrowth microstructures and reaction mechanisms. American Mineralogist, 66, 1107–1134.

Veblen, D.R., and Bish, D.L. (1988) TEM and X-ray study of orthopyroxene megacrysts: Microstructures and crystal chemistry. American Mineralogist, 73, 677–691.

Wang, C., and Zhang, H. (1991) Characteristic thermal spectra and mechanisms of thermal transformation of nephrites. Acta Mineralogica Sinica, 11, 251–257 (in Chinese).

Williams, H., Turner, F.J., and Gilbert, C.M. (1958) Petrography: An introduction to the study of rocks in thin sections, p. 177–198. Freeman and Company, San Francisco, California.

Xu, H., Luo, G., and Xu, N. (1988) TEM study of phase transformation from amphibole to pyroxene. In Proceedings of the 2nd National Conference on Microbeam Analysis, p. D9–12. Chinese Society of Mineralogy, Petrology and Geochemistry, Guiyang.

Manuscript received April 20, 1995
Manuscript accepted April 29, 1996